CHEMICAL ENGINEERING TRANSACTIONS

VOL. 62, 2017

A publication of AIDIC
The Italian Association of Chemical Engineering
Online at www.aidic.it/cet

Guest Editors: Fei Song,Haibo Wang, Fang He
Copyright © 2017, AIDIC Servizi S.r.l.
ISBN978-88-95608- 60-0; **ISSN** 2283-9216

DOI: 10.3303/CET1762044

Impact of Cu Content on Corrosion Property of Zn20Sn Lead-free Solder

Qiumin Wang*, Hongxia Mou

Shandong Polytechnic, No. 23000, 10th East Road, Jinan 250104, China
wangqiumin72@126.com

By alloying principle, different contents of Cu were added in the matrix Zn20Sn filler metals to form a new type of alloy, the effects of Cu contents on the Zn20Sn solder alloy corrosion resistance were studied. The results show that when the Cu content is less than 4%, with the increase of Cu content, Zn20SnxCu solder alloy corrosion potential increased and corrosion rate reduced gradually, the corrosion resistance of solder alloy increased. When the Cu content is more than 4%, with the increase of Cu content, Zn20SnxCu solder alloy corrosion potential reduced and corrosion rate increased gradually, the corrosion resistance of solder alloy reduced. Main products on the corrosion surface of Zn20SnxCu are $Zn_5(OH)_8Cl_2.H_2O$ and ZnO. Under the consideration of the corrosion performance of Zn20SnxCu, the best addition amount of Cu is 4%.

1. Introduction

High-Pb soft solder is widely applied in power semiconductor package, but Pb has a great hazard to the human body and environment. For this reason, people have raised more concern about lead-free HT solder (Dai et al., 2005, Hu et al., 2005). To fabricate reliable electron components for high-density packaging technology and high-temperature operations, the HT solders become more and more popular. Today, the HT lead-free solder alloy series under development include Au-Sn, Bi-Ag, Zn-Sn, etc. Among the candidate HT lead-free solder alloy series, the Au-20Sn solder can be used at a temperature of 270 ° C (Kim et al., 2009, Lalena et al., 2002). Since Au is expensive, and prone to form a hard and brittle Au-Sn IMC (intermetallic compound), Au-based solder will struggle to leave its infancy (Li et al., 2012). Bi-Ag solder joint has less adhesive strength, microhardness and conductivity than Pb-5Sn. Zn-Sn HT lead-free solder has an appropriate fusion range and a good thermal / conductivity. As cheap it is, it has been regarded as a new one of the most promising HT lead-free solder (Liu et al., 2008, Wang et al., 2010). Zn-based alloy is poor in terms of corrosion resistance, oxidation resistance and wettability, which has hindered it from widespread application. KIM et al explored how the Zn-xSn (x=20wt%, 30wt% and 40wt%) solder alloy reacted with Cu substrate interface, with shear strength of 30-34MPa higher than Pb-5Sn (Kim et al., 2009). Kang et al. probed into Zn- (4-6) wt% Al- (1-5) wt% Cu and other HT solders. The results reveal that the additive Al can extend the spread area and resistivity of the solders. Additive Cu element can improve the hardness and the tensile strength of solder (Kang et al., 2009, Mendoza et al., 2000).
Corrosion resistance is an important property of solder alloy. It has not been reported about how the additive Cu affects the corrosion resistance of Zn20Sn solder. In this paper, by applying the alloying principle, Cu is added to solder matrix in different contents. Using the electrochemical corrosion, uniform corrosion and immersion tests, we delve deeper into Zn20SnxCu lead-free solder corrosion behavior and mechanism.

2. Test materials and methods

2.1 Alloying preparation

The raw materials used in the test are 70Sn30Cu alloy, arsenic-free Zn particles with 99.93% purity, Sn particles with 99.9% purity and Cu flake with 99.5% purity. The composition proportions of solders are shown in the Table 1. The raw materials are weighed at a ratio of design, and placed into a crucible. Keep the temperature at 800°C in a box type resistance furnace for 20min. In order to prevent the solder from

oxidization, KCl and NaCl are used as a protective agent and weighed at a ratio of 2: 1. The total mass of the protective agent is 20% -30% of the solder. In order to ensure the uniformity of the alloy, it shall be stirred constantly during melting process.

Table 1: Composition of alloy (wt, %)

Composition	70Sn30Cu	Sn	Zn
Zn20Sn	0	20	80
Zn20Sn2Cu	6.667	15.3333	78
Zn20Sn4Cu	13.333	10.667	76
Zn20Sn6Cu	20	6	74
Zn20Sn8Cu	26.667	1.333	72

2.2 Corrosion potential measurement

The solder is prepared into a block of 10.2mm×10.2mm×15 mm. The working face of the sample is polished by 180 #, 320 #, 600 #, 800 #, 1000 #, 1500 # and 2000 # waterproof abrasive paper in turn into a square with a side length of 10 mm, degrease and wash it out with acetone, alcohol and other reagents, and then clean its surface with ultrasonic waves for 30 minutes to remove impurities, dust and the like. Cu wire is wound on the non-working face of the solder. To ensure that the area of working face reaches $1cm^2$, the other parts of the solder are first cured using phthalic acid anhydride, ethylene diamine and epoxy, and then wrapped with the raw material band to make sure that the area of the remaining face is $1cm^2$.
In the electrochemical corrosion test, the electrochemical workstation CH I600C "Tafel Curve" electrochemical test system is used. A three-electrode system measures the anode polarization curve of solder in the mass fraction of 3.5% NaCl using the potentiodynamic scanning method. Auxiliary electrode is a carbon rod, and the reference electrode is a saturated calomel electrode. Scan range of potential falls within -1500 mV ~ -500 mV at a scan rate of 1 mV/s and at room temperature.

2.3 Determination of corrosion rate

The maceration test is conducted in accordance with the machinery industry standard JB/T 7901-1999 *Metals materials - Uniform corrosion - Methods of Laboratory Immersion Testing*. The selected sample plate, 50mm×25mm×3mm, is polished, degreased and washed. After drying, a Vernier caliper is used for measuring the dimension of block sample, weigh M1 with an electronic balance. In the maceration solution with mass fraction of 3.5% NaCl, the etching time lasts for 14 days and the solution is changed every 5 days. The whole etching process is carried out at room temperature. The sample is removed after a predefined time interval, first flush it with water, wipe off the corrosion products with a brush, eraser, etc., and then make an ultrasonic cleaning. After the sample is cleaned, thoroughly de-oil it and wash it with water, etc., then degrease with reagents such as acetone and alcohol without chlorine ions, store it in a desiccator immediately after drying. It is weighed as M_2 with an electronic balance at a room temperature. The erodent corrosion rate R can be calculated by the formula (1). The above test is repeated three times for each solder alloy, and the average of three corrosion rates is evaluated as the corrosion rate of the solder alloy.

$$R = \frac{8.76\times10^{7}\times\left(M_1 - M_2\right)}{STD} \tag{1}$$

Where: R-corrosion rate (mm/a); M1-the mass (g) of the sample before the test; M2-the mass (g) of the sample after the test; S- the total area (mm/a) of the sample; D-the density (kg / m3) of the material.

3. Sample results and analysis

3.1 Impact of Cu on Zn20Sn solder corrosion potential

The electrochemical corrosion polarization curve and the corrosion potential of Zn20SnxCu solder alloy are shown in Figure 1. Zn20SnxCu solder alloy is eroded uniformly; there is an obvious passivation area caused by the formation of the dense corrosion products on the surface of solder alloy. According to the corrosion potential curve, we can learn that the Zn20Sn solder has the lowest corrosion potential, -1.2477V, and the worst corrosion resistance. When the volume of Cu addition is less than 4%, the corrosion potential of Zn20SnxCu solder alloy increases gradually with the increasing of Cu addition, and the corrosion resistance gradually strengthens. When the volume of Cu addition reaches 4%, the corrosion potential of Zn20Sn4Cu solder alloy climbs up to the top, -1.1785V, and 5.5% higher than that of matrix alloy. When Cu content is more than 4%, the corrosion potential of Zn20SnxCu solder alloy decreases gradually with the increasing of Cu addition, while the corrosion resistance decreases a little.

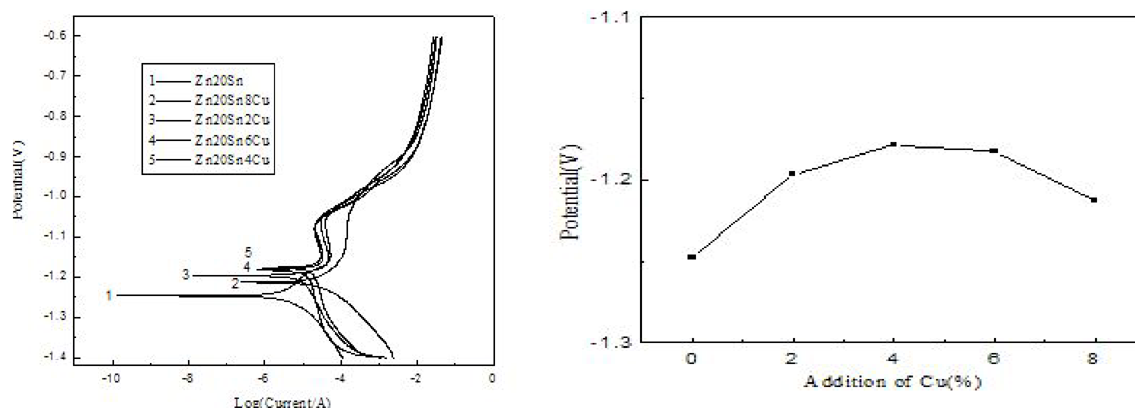

(a) Zn20SnxCu solder polarization curve (b) Zn20SnxCu solder corrosion potential

Figure 1: Polarization curves obtained from NaCl solution and the potential of Zn20SnxCu solder alloys.

The microstructure of Zn20SnxCu solder alloy is shown in Figure 2. We can learn by the solder energy spectrum and XRD interpretation of results that the Zn20Sn solder alloy structure is α-Zn, SnZn phase and Zn-rich phase. Since the electrode potential of Zn monomer is -0.763V, lower than that of Sn electrode, the corrosion process of Zn20Sn solder is such that Zn and Sn form the primary batterys, among which the Zn element is corroded as the anode. Zn20Sn solder alloy contains a mass of α-Zn. Zn in the SnZn phase can also bond with Sn to form the primary battery by redox reaction. So the corrosion potential of Zn20Sn is lowest. Additive Cu element makes the corrosion potential of the solder alloy increases because the addition of Cu modifies the microstructure of the solder. The erosive α-Zn phase does not exist in the Zn20SnxCu solder structure any more, while white structure SnZnCu phase with reticular distribution and gray matrix structure ε-$CuZn_5$ intermetallic compound exist instead. The addition of SnZnCu phase reduces the relative contain of monomer Zn, which helps improve the corrosion resistance, and the corrosion potential of the Zn20SnxCu solder alloy increases due to the increased corrosion resistance of the ε-CuZn5 intermetallic compound.

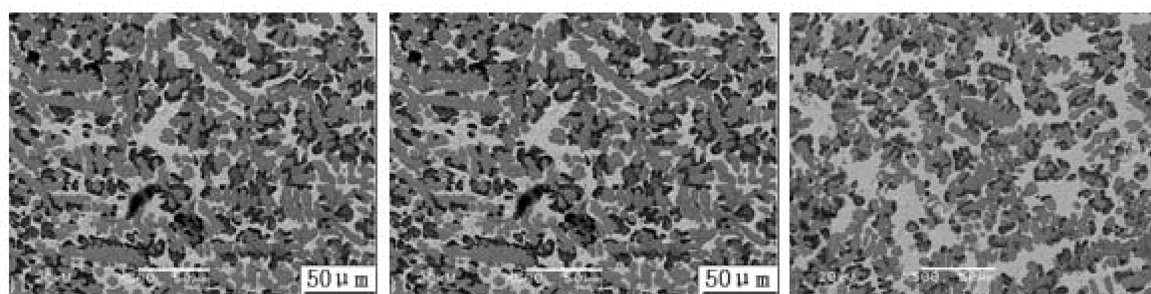

(a) Zn20Sn (b) Zn20Sn4Cu (c) Zn20Sn8Cu

Figure 2: SEM photograph of Zn20SnxCu solder alloys

3.2 Impact of Cu on Corrosion Rate of Zn20Sn Solder

The impact of Cu on the Zn20Sn solder alloy corrosion rate is shown in Figure 3. We can see that Zn20Sn solder corrosion rate is maximum, 0.112mm/a. When the content of Cu is less than 4%, the corrosion rate of Zn20SnxCu solder alloy decreases with the increasing of Cu content. The corrosion rate of Zn20Sn4Cu solder alloy is lowest (0.079 mm / a), 29.5% lower than that of the matrix alloy. When Cu content is more than 4%, the corrosion rate of Zn20SnxCu solder alloy increases gradually with the increasing of Cu content. The corrosion rate of Zn20Sn8Cu solder alloy is 0.110mm / a, but still lower than that of matrix alloy. It follows that the addition of Cu element to Zn20Sn matrix can significantly improve the corrosion resistance of Zn20Sn solder. Zn20Sn4Cu solder corrosion surface is shown in Figure 4. It is obvious that there are plenty of large and small, white, convex tumorous substances on the surface of the corroded specimen, on the surface of

each of which many small tumors grow, and are uniformly distributed on the surface of the black matrix. As shown in Figure 5 and 6, it is known from the analysis of energy spectrum, XRD that the main products on the corrosion surface are $Zn_5(OH)_8Cl_2\,H_2O$, Na-Cl, ZnO, tumorous substances of NaCl and $Zn_5(OH)_8$- Cl_2H_2O and ZnO on the surface of black matrix. In NaCl aqueous solution, NaCl is reserved on the surface of corrosion products and coalesces with the Zn_5- $(OH)_8Cl_2H_2O$ to form a tumor-like substance. Zn_5- $(OH)_8Cl_2H_2O$ is a compound produced during corrosion. On the surface of solder matrix, Zn element content is relatively large, and prone to be oxidized into ZnO. In the atmosphere, Zn surface easily forms porous ZnO, but in humid atmosphere or in the environment of halide, further generates ε-$Zn(OH)_2$, $Zn_5\,(C0_3)_2(OH)_6$, $Zn_5(OH)_8Cl_2H_2O$.

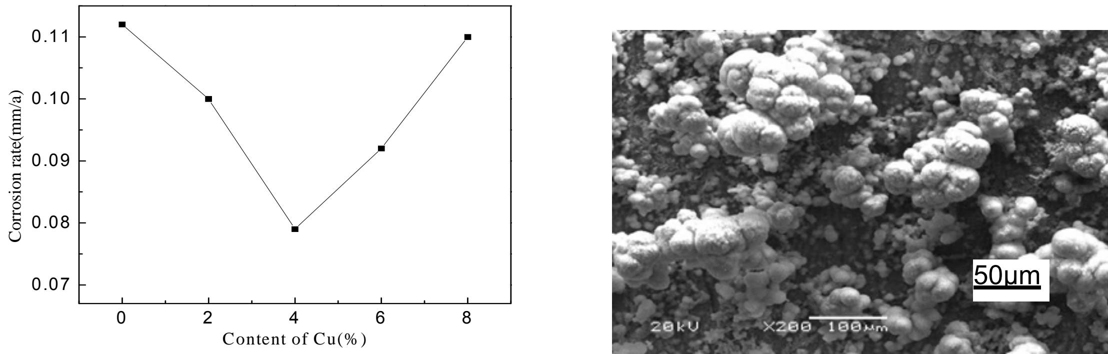

Figure 3: Corrosion rate of Zn20SnxCu solder alloy Figure 4: The corrosion pattern of Zn20Sn4Cu solder alloy

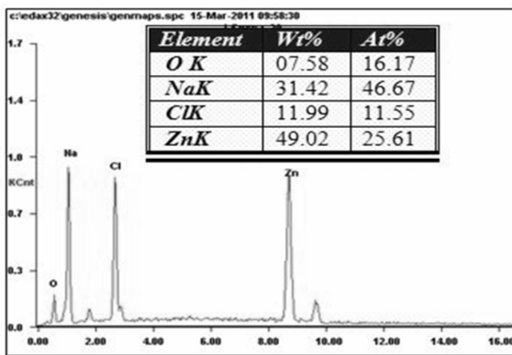

Element	Wt%	At%
O K	07.58	16.17
NaK	31.42	46.67
ClK	11.99	11.55
ZnK	49.02	25.61

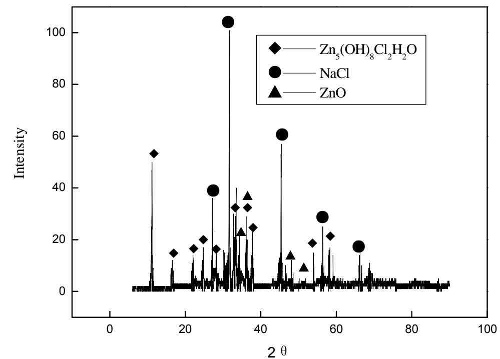

Figure 5: EDX of Zn20Sn4Cu solder alloy

Figure 6: XRD of Zn20Sn4Cu solder alloy

The SEM of Zn20SnxCu solder alloy is shown in Figure 7. A bulk of water-caltrop-like particles heap up on the entire surface of Zn20Sn solder, evenly distributed and with larger diameters, while partially distributed on the surface of Zn20Sn4Cu solder as some clusters. The particle size decreases, so does the number of them; such particles are also evenly distributed on the surface of Zn20Sn8Cu solder with uniform and small size, which shows that the addition of Cu element in the Zn20Sn matrix obviously changes the morphology of corrosion products on the surface of the solder.

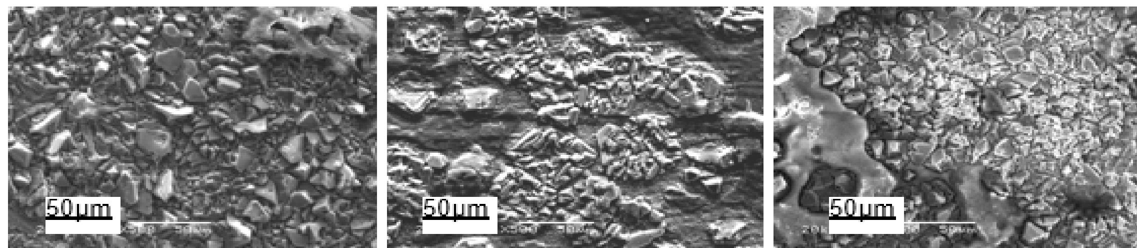

(a) Zn20Sn (b) Zn20Sn4Cu (c) Zn20Sn8Cu

Figure 7: The corrosion pattern of Zn20SnxCu solder alloys

The Zn20Sn solder corrosion surface energy spectrum is analyzed as shown in Figure 8 (a) below. The main components of corrosion products are Zn, O, but there is no Sn element. The Zn instead of Sn in Zn20Sn solder is corroded. The water-caltrop particles are ZnO. Zn20Sn2Cu solder corrosion surface energy spectrum is analyzed as shown in Fig. 8 (b) below. Water-calrop-like corrosion products are mainly composed of Zn, O, but Sn element is none. Matrix is shown in Fig. 8 (c), its main components include Zn, O, Sn and Cu. We can speculate that the water-caltrop-like particles are ZnO, and the matrix solder is composed of ZnO.

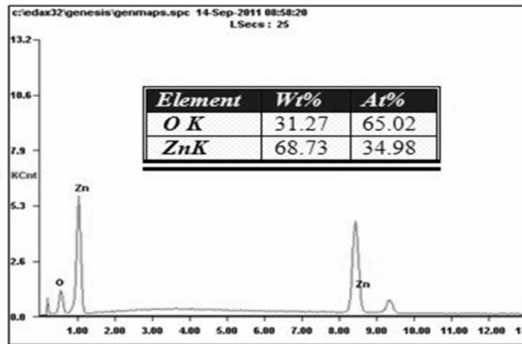

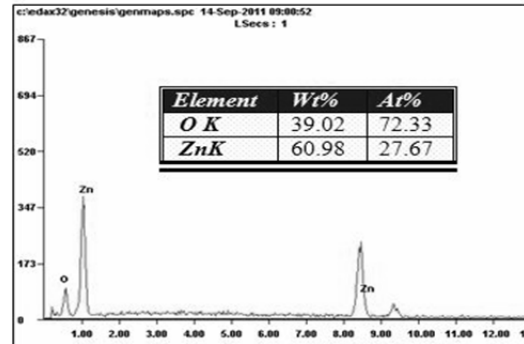

(a) Zn20Sn

(b) Zn20Sn2Cu water-caltrop-like corrosion products

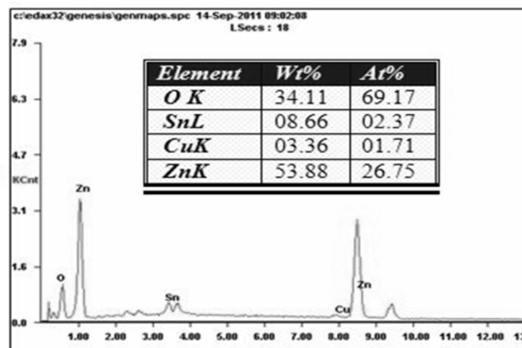

(c) Zn20Sn2Cu matrix

Figure 8: EDX of Zn20SnxCu solder alloy

As described above, during the corrosion process of Zn20Sn solder, the α-Zn and SnZn phases and Sn constitute the primary battery where they have a redox reaction. The Zn element is corroded as anode due to the low electrode potential at a maximum corrosion rate; After Cu element is added, the corrosion process of the solder is such that SnZnCu phase and $CuZn_5$ constitute the primary battery, with Zn as the anode, ε-$CuZn_5$ intermetallic compound as the cathode, and the potential difference is higher. The driving force for the redox reaction is strong to make the reaction easier. However, in relation to Zn20Sn solder, the amount of Zn element decreases and mainly exists in the form of SnZnCu phase. The Sn element makes the reaction process retard and even reduces its contact area with Zn, thus the corrosion rate delays. As shown in Fig. 2 (b), the ε-$CuZn_5$ intermetallic compounds in Zn20Sn6Cu take on ridge shape, more than those in the Zn20Sn2Cu solder, and the volume fraction is also maximum; The ε-$CuZn_5$ intermetallic compound has a high potential, and is not corroded, but reduces the relative contain of Zn in the solder. The contain of the black Zn-rich phase also decreases a little, that is to say, the contain of the Zn element in the Zn-rich phase decreases a lot, so that the corrosion rate is lower than that of the Zn20Sn2Cu solder. The SnZnCu phases of Zn20Sn8Cu solder alloy climb up to the maximum. The volume percentage of ε-$CuZn_5$ intermetallic compound is the minimum, so that the content of Zn element increases while the corrosion potential decreases. In view of the corrosion potential, Zn20Sn4Cu solder alloy has a good corrosion resistance.

4. Conclusions

(1) Zn20SnxCu solder alloy is uniformly corroded; when additive Cu is less than 4%, the corrosion potential of Zn20SnxCu solder alloy gradually increases with the increasing of additive Cu, and the corrosion resistance also gradually increases. The corrosion potential of Zn20Sn4Cu solder alloy is highest, -1.1785V, and 5.5% more than the matrix alloy. When additive Cu is more than 4%, the corrosion potential of Zn20SnxCu solder alloy decreases gradually with the increasing of additive Cu, and the corrosion resistance decreases a lot.
(2)The corrosion rate of Zn20Sn solder is highest, i.e. 0.112mm / a. When the content of Cu is less than 4%, the corrosion rate of Zn20SnxCu solder alloy decreases with the increasing of Cu content. The corrosion rate of Zn20Sn4Cu solder alloy is lowest, i.e. 0.079 mm / a, and 29.5% lower than that of the matrix alloy. When Cu content is more than 4%, the corrosion rate of Zn20SnxCu solder alloy increases gradually with the increasing of Cu content. The corrosion rate of Zn20Sn8Cu solder alloy is 0.110mm / a, but still lower than that of matrix alloy.
(3)The addition of Cu element on Zn20Sn matrix can help significantly improve the corrosion resistance of Zn20Sn solder. The staple product on Zn20SnxCu corrosion surface is $Zn_5(OH)_8Cl_2H_2O$, ZnO. As far as the corrosion rate is concerned, the optimal Cu additive content in Zn20SnxCu solder alloy is 4%.

Reference

Dai J. H., Liu X. Z., Chen L.B., 2005, Legislation and Development of Lead-free Solders (in Chinese), ZHUAN LUN YU ZONG SHU, 1, 7-12, DOI: 10.16107/j.cnki.mmte.2005.01.002

Hu Z. T., He Q. J., Xu D. R., 2005, Research and Development Trend of Lead-free Solder alloy in home and abroad (in Chinese), Welding Technology, 3, 4-6, DOI: 10.13846/j.cnki.cn12-1070/tg.2005. 03.002

Kim S., Kim K. S., Suganuma K., Izuta G., 2009, Interfacial reactions of Si die attachment with Zn-Sn and Au - 20Sn high temperature lead-free solders on Cu substrates, Journal of Electronic Materials, 6, 873-883, DOI: 10.1007/s11664-009-0770-y

Lalena L. N., Dean N. F., Weiser M. W, 2002, Experimental investigation of Ge-doped Bi-11Ag as a new Pb-free solder alloy for power die attachment, Journal of Electronic Materials, 11, 1244-1249

Li J. L., Tan K. K., Zhang Z. H., Hu Q., Luo J., Li S. J., 2012, Application of AuSn Alloy in Electronic Package and Its Research Progress (in Chinese), Microelectronics, 4, 539-546

Liu M. F., Chen P., 2008, Study of Zn-based brazing alloy with intermediate melting temperature (in Chinese), MATERIALS RESEARCH AND APPLICATION, 2, 126-128

Wang H. L., Lu W. J., Yu W. Y., Li P., 2010, Preparation and property of new composite zinc-based filler metal (in Chinese), Welding Technology, 1, 50-52, DOI: 10.13846/j.cnki.cn12-1070/tg.2010.01.008

Kim S., Kim K. S., Kim S. S., 2009, Improving the reliability of Si die attachment with Zn – Sn – based high-temperature Pb-free solder using a TiN diffusion barrier, Journal of Electronic Materials, 12, 2 668-2675.

Kang N., Na H. S., Kim S. J., 2009, Alloy design of Zn–Al–Cu solder for ultra-high temp- eratures, Journal of Alloys and Compounds, 467, 246–250.

Mendoza A., Corvo F., 2000, Outdoor and indoor atmospheric corrosion of non-ferrous metals, Corrosion. Science. 42, 1123-1147